PHYSICAL REVIEW D VOLUME 23, NUMBER 7 1 APRIL 1981

# Rapid Communications

*The Rapid Communications section is intended for the accelerated publication of important new results. Manuscripts submitted to this section are given priority in handling in the editorial office and in production. A Rapid Communication may be no longer than $3\frac{1}{2}$ printed pages and must be accompanied by an abstract. Page proofs are sent to authors, but, because of the rapid publication schedule, publication is not delayed for receipt of corrections unless requested by the author.*

## Quantum-chromodynamic predictions for deep-inelastic $J/\psi$ production

D. W. Duke and J. F. Owens
*Physics Department, Florida State University, Tallahassee, Florida 32306*
(Received 22 October 1980)

New data on deep-inelastic $J/\psi$ production by muons show a large inelastic cross section. We show that the energy, $Q^2$, and $p_T$ dependences of both the elastic and inelastic data are in agreement with the predictions of the photon-gluon-fusion model extended to include higher-order corrections. A striking correlation between the lepton and $J/\psi$ scattering planes is predicted which tests further the relevance of this perturbative production mechanism.

The photon-gluon-fusion model,[1] based on the subprocess $\gamma g \to c\bar{c}$, has been used to calculate both charm and $J/\psi$ photoproduction cross sections. In the latter case the subprocess cross section is integrated over the $c\bar{c}$ mass from $2m_c$ to the threshold for $D\bar{D}$ meson-pair production and divided by (approximately) the number of $c\bar{c}$ bound states below the $D\bar{D}$ threshold.[2] This model has also been extended to include virtual photoproduction[3] and gives a good description of the dependence of the *elastic* $J/\psi$ leptoproduction cross section on the photon mass squared $(-Q^2)$ and the laboratory energy $\nu$.

Recent data have revealed that the *inelastic* production of $J/\psi$ is at least as large as the elastic production for photon laboratory energies $\nu \gtrsim 100$ GeV. In this paper we show that the photon-gluon-fusion model, extended to include the higher-order subprocesses $\gamma g \to c\bar{c}g$ and $\gamma q \to c\bar{c}q$, yields predictions which are in agreement with the $\nu$, $Q^2$, and $p_T$ dependences and relative normalization of the elastic and inelastic $J/\psi$ production cross sections.[4] In addition we also predict a strong correlation between the lepton and $J/\psi$ scattering planes. The experimental verification of this correlation would test both this perturbative production mechanism and the gluon spin-parity.

The Feynman diagrams corresponding to the subprocesses $\gamma g \to c\bar{c}g$ and $\gamma q \to c\bar{c}q$ are shown in Fig. 1. We have calculated the corresponding squared matrix elements $T_{\mu\nu}$ using the algebraic-manipulation program SCHOONSCHIP.[5] The virtual-photon differential cross section is then given by

$$\frac{1}{\Gamma}\frac{d\sigma}{dQ^2\,d\nu\,dz\,dp_T{}^2} = \sum_a \int G_{a/p}(x, Q^2+M^2)\frac{\nu^2(1-M^2/\hat{s})(\frac{1}{4}-m_c{}^2/M^2)^{1/2}}{(4\pi)^5 8xs[E^2+(E-\nu)^2]} L_{\mu\nu}T_{\mu\nu}\delta(p_T{}^2-(\hat{s}-M^2)^2\sin^2\theta/4\hat{s})$$
$$\times\,\delta(z-\tfrac{1}{2}[1+M^2/\hat{s}+(1-M^2/\hat{s})\cos\theta])\,dx\,dM^2 d\cos\theta\,d\phi\,d\Omega_{12}\ , \qquad (1)$$

with the tensor $L_{\mu\nu}=4l_\mu l_\nu/q^2-g_{\mu\nu}$ where $l_\mu$ is the incident-lepton four-vector with laboratory energy $E$. Also $s$ is the invariant mass squared of the photon–hadron-target system whereas $\hat{s}$ is the invariant mass squared of the photon-parton system where the parton $a$ has target-momentum fraction $x$ and a scale-violating probability distribution $G(x,Q^2)$. The $c\bar{c}$ system has invariant mass $M$, transverse momentum $p_T$, energy fraction $z=E_{c\bar{c}}/\nu$ in the laboratory, and scattering angle $\theta$ in the photon-parton center-of-mass system. $\Omega_{12}$ is the direction of a charmed quark (of mass $m_c$) in the $c\bar{c}$ rest frame. Finally, $\phi$ is

 

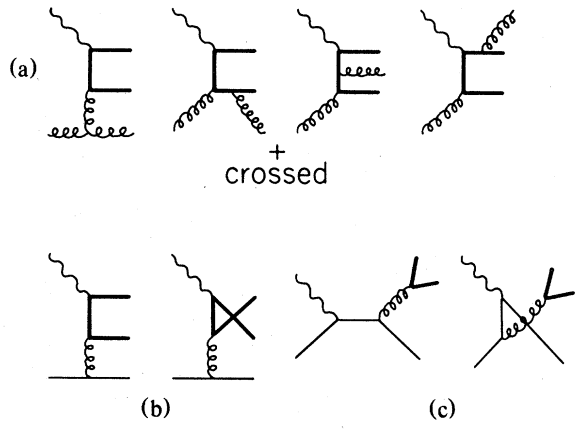


FIG. 1. Feynman diagrams for the subprocesses (a) $\gamma g \to c\bar{c}g$ and (b),(c) $\gamma q \to c\bar{c}q$. The heavy lines denote the charm quarks.

the azimuthal angle between the lepton and $c\bar{c}$ $(J/\psi)$ scattering planes and $\Gamma$ is a virtual-photon flux factor

$$\Gamma = \alpha(\nu - Q^2/2m_p)/2\pi Q^2 E^2(1-\epsilon)$$

with

$$\epsilon = [4E(E-\nu) - Q^2]/\{2[E^2 + (E-\nu)^2] + Q^2\}$$

and $m_p$ the target mass. In obtaining Eq. (1) the limit $\nu^2 > Q^2$ has been imposed. The $Q^2 \to 0$ limit of Eq. (1) reproduces the results of Ref. 4.

Our numerical calculations have used the scale-violating quark distributions from Ref. 6 and a gluon distribution

$$xG(x, Q^2 = 4\ (\mathrm{GeV}/c)^2) = 0.92(1+9x)(1-x)^4$$

from Ref. 7. The quantity $Q^2 + M^2$ was used in computing the scaling violations for these functions, as indicated in Eq. (1).

In order for the predictions obtained using Eq. (1) to be valid, it is necessary to avoid those kinematic regions for which the subprocess matrix elements contain singularities. For $p_T^2 \neq 0$ there are no such singularities. For $p_T^2 = 0$ there are two possible divergences corresponding to $\cos\theta = \pm 1$. If $\cos\theta = +1$ then examination of the second $\delta$ function in Eq. (1) shows that $z = 1$. The diagrams in Fig. 1(b) and some of those in Fig. 1(a) possess this singularity. On the other hand, if $\cos\theta = -1$, then $z = M^2/\hat{s}$. In this latter instance if $Q^2 \neq 0$ there are no divergences while for $Q^2 = 0$ the second diagram in Fig. 1(c) contains a singularity. Therefore, there are two singularity-free regions of interest: (1) $p_T^2 > 0$ for any $z$ and $Q^2$, and (2) $p_T^2 \geq 0$, $Q^2 > 0$, and $z < 1$.

We have used Eq. (1) to study the joint $z$ and $p_T$ distributions as functions of $\nu$ and $Q^2$. The most striking feature of the $z$ distributions at fixed $p_T \neq 0$ is a peak near $z = 1$ with a long tail extending to lower $z$ values. The location of the peak in $z$ moves to lower $z$ values as the $p_T$ is increased. This is due to a kinematic cutoff which forces $z$ to be less than 1 for finite $p_T$:

$$z < z_{\max} = \tfrac{1}{2}\{1 + M^2/s + [(1 - M^2/s)^2 - 4p_T^2/s]^{1/2}\}\ .$$

This upper limit corresponds to $x = 1$ and, therefore, the cross section vanishes at this end point due to the vanishing of the parton distributions.

The European Muon Collaboration has published data on both elastic[8] and inelastic[9] $J/\psi$ production. They have defined elastic events as those with recoil hadronic energy below 5 GeV in the laboratory, corresponding to $z > 1 - (5\ \mathrm{GeV}/\nu)$. These data include the integrated cross sections extrapolated to $Q^2 = 0$ and also the $p_T$ distributions for both the elastic and inelastic events; the joint $z$ and $p_T$ distributions are not yet available. These data show a large inelastic cross section which exceeds the elastic one above $\nu \simeq 100$ GeV.

The inelastic cross section at fixed $\nu$ and for $Q^2 \neq 0$ may be obtained by a straightforward integration of Eq. (1) over $p_T$ and $z$ with the above mentioned $z$ cut. For $z < 1$, the only potential singularity is that in the second diagram of Fig. 1(c) and this occurs only at $Q^2 = 0$; for the $Q^2$ values used in this calculation the contribution was completely negligible. Now, the inelastic cross section given in Ref. 9 has been extrapolated to $Q^2 = 0$ using measurements at finite $Q^2$. By following a similar procedure the calculation of the inelastic cross section extrapolated to $Q^2 = 0$ becomes insensitive to the contributions of the diagram in Fig. 1(c).

The calculation of the elastic cross section is in principle somewhat more complicated. Equation (1) should be integrated over the region allowed by the elastic $z$ cut. This includes the divergence at $p_T = 0$, $z = 1$. There are also contributions from various virtual diagrams at this point which should be included. The mass singularities could then be factored off, leaving a finite result for the elastic cross section. In practice, however, the answer for the elastic cross section can be obtained to leading-logarithm accuracy by using the lowest-order subprocess, $\gamma g \to c\bar{c}$, with a scale-violating gluon distribution. This leading-logarithm approximation will reproduce the results of the full calculation up to various nonleading corrections. In Fig. 2(a) we show the results of such a leading-logarithm calculation for the elastic cross section. The predictions have been normalized by dividing by a factor of 4.5.[12]

The predictions for the inelastic cross section, obtained as discussed above, are shown in Fig. 2(b). In these and all subsequent predictions an incident lepton energy of 280 GeV was used and the normaliza-

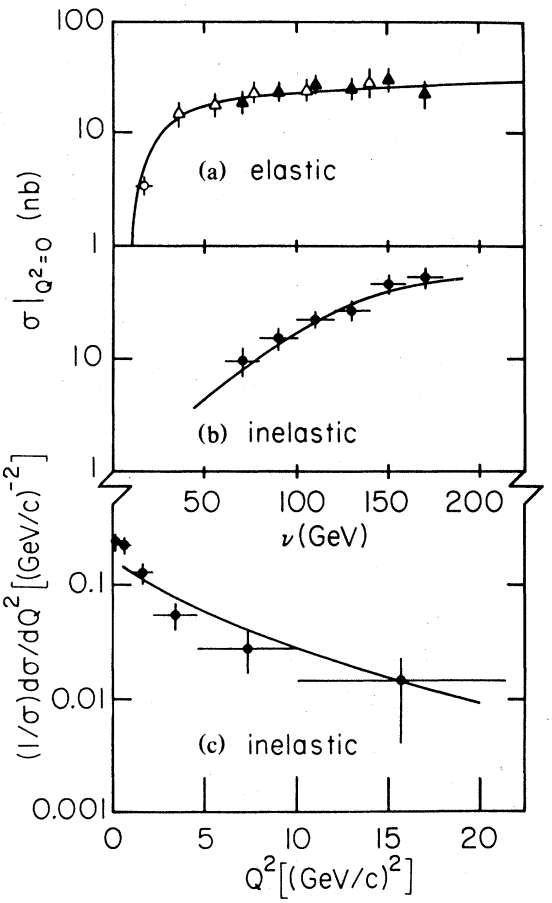


FIG. 2. Comparison between the theoretical predictions and data for (a) elastic cross section at $Q^2=0$, (b) inelastic cross section extrapolated to $Q^2=0$, and (c) the normalized $Q^2$ distribution for the inelastic cross section. The data are from Ref. 9 (solid triangles and solid circles), Ref. 10 (open triangles), and Ref. 11 (open circle).

tion factor of 4.5 was kept fixed. The rapid rise of the inelastic cross section with increasing $\nu$ is due to the $\nu$-dependent $z$ cut used in the experimental definition of the inelastic events. At higher $\nu$ values more of the $z$ peak is included in the cross section. The flattening out of the cross section at high $\nu$ is a manifestation of the turnover of the $z$ distribution which was discussed previously. At this point it should be stressed that for increasing $\nu$ one can come arbitrarily close to $z=1$ and, therefore, the inelastic cross section can become arbitrarily large, signaling a breakdown of perturbation theory. We note that a complete analysis of the region very near $z=1$ must include a resummation of the large logarithms encountered there. However, due in part to the vanishing of the gluon distribution at $z=z_{\max}$, there is no sign of these divergences in Fig. 2(b). Indeed, the predictions agree with the data over the entire $\nu$ range shown.

In Fig. 2(c) we show that the $Q^2$ dependence of the inelastic cross section is well described by the higher-order subprocesses. In Ref. 3 it was shown that the $\gamma g \rightarrow c\bar{c}$ subprocess gives a good description of the $Q^2$ dependence of the elastic cross section.

In Fig. 3 the predictions of the model are compared with data[8,9] for the elastic, inelastic, and total $J/\psi$ $p_T$ distributions. The lowest-$p_T$ data points have been corrected for the coherent contribution arising from the use of an iron target. The relative normalizations of the curves are fixed by the $z$ cut used in defining the elastic/inelastic separation. The overall normalization has been kept fixed using the results from Fig. 2(a). The predictions agree well with the distinctive differences in shape between the elastic and inelastic curves. The steeper falloff of the elastic cross section occurs because there is a kinematic cutoff at the $p_T$ value where $z_{\max}$ is equal to the lower limit on $z$ for the elastic-cross-section definition.

In deep-inelastic scattering the polarization of the virtual photon is determined by the scattering angle and momentum transfer at the lepton vertex and, furthermore, the orientation of the photon polarization vector is related to the orientation of the lepton

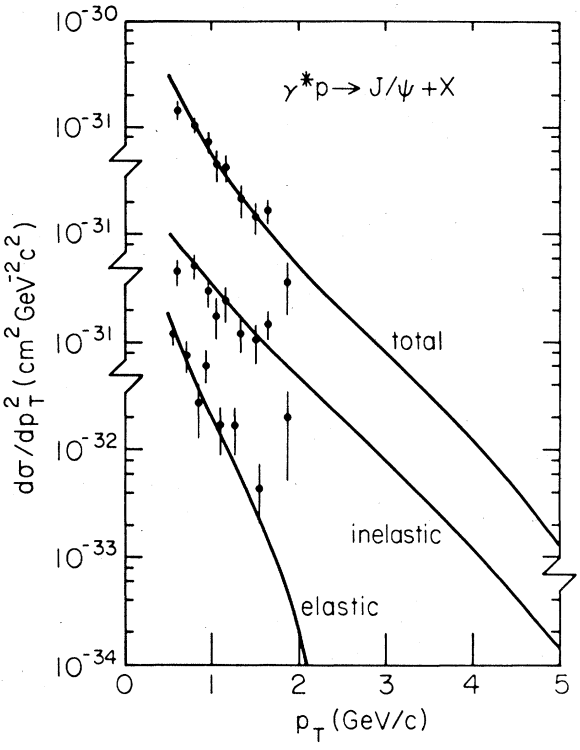


FIG. 3. Comparison between the theoretical predictions and the data (Refs. 8 and 9) for the $J/\psi$ $p_T$ distribution. Both theory and data are integrated over $Q^2$ and averaged over the range $60 \leq \nu \leq 180$ GeV.

scattering plane. The dependence of the cross section on the photon polarization then shows up as a correlation between the lepton and $J/\psi$ scattering planes. In a coordinate system where the $z$ axis is along the virtual photon's momentum vector, let $\phi$ be the azimuthal angle between the two scattering planes. Then one can define a linearly polarized photon asymmetry $\Sigma$ by

$$(1/\sigma)d\sigma/d\phi=(1/2\pi)(1-\Sigma\cos 2\phi) \quad . \tag{2}$$

For the process being considered here $\Sigma$ has kinematic zeroes at $Q^2$ and $p_T=0$ since the lepton and $J/\psi$ scattering planes, respectively, are undefined at these points. We have calculated $\Sigma$ in the region $Q^2>1$ $(\mathrm{GeV}/c)^2$ and $p_T{}^2>0.5$ $(\mathrm{GeV}/c)^2$. In this region we find $\Sigma\simeq 0.25\pm 0.05$, where the error reflects the uncertainty in our Monte Carlo calculation. We have separately investigated the $\nu$, $Q^2$, and $p_T$ dependences of $\Sigma$ and find little dependence on $\nu$ or $Q^2$ in the above region. There is a slight decrease with increasing $p_T$ above 1 GeV/$c$ with the above $Q^2$ cut. In addition we have studied the dependence of $\Sigma$ on the spin-parity and coupling of the gluon. Virtually identical results were obtained with an Abelian vector gluon while both scalar and pseudoscalar gluons yield $\Sigma=0$ in the region defined above.

We have shown that quantum-chromodynamic perturbation theory can be used to give a good description of the available data for the $\nu$, $Q^2$, and $p_T$ dependences of both the elastic and inelastic $J/\psi$ leptoproduction cross sections. In addition, the prediction of the large asymmetry $\Sigma$ provides a new test of the theory that can be performed with data which should soon become available.

One of the authors (J.F.O.) wishes to acknowledge useful discussions with D. M. Scott, J. P. Leveille, and T. Weiler. This work was supported in part by the U.S. Department of Energy.

[1]L. M. Jones and H. W. Wyld, Phys. Rev. D 17, 759, 2332 (1978).
[2]H. Fritsch, Phys. Lett. 67B, 217 (1977).
[3]T. Weiler, Phys. Rev. Lett. 44, 304 (1980); V. Barger, W. Y. Keung, and R. J. N. Phillips, Phys. Lett. 91B, 253 (1980).
[4]The analogous calculation for real photons can be found in D. W. Duke and J. F. Owens, Phys. Lett. 96B, 184 (1980).
[5]H. Strubbe, Comp. Phys. Comm. 8, 1 (1974).
[6]J. F. Owens and J. D. Kimel, Phys. Rev. D 18, 3313 (1978).
[7]R. P. Feynman, R. D. Field, and G. C. Fox, Phys. Rev. D 18, 3320 (1978).
[8]J. J. Aubert *et al.*, Phys. Lett. 89B, 267 (1980).
[9]J. J. Aubert *et al.*, CERN Report No. EP/80-84, 1980 (unpublished).
[10]A. R. Clark *et al.*, Phys. Rev. Lett. 43, 187 (1979).
[11]U. Camerini *et al.*, Phys. Rev. Lett. 35, 483 (1975).
[12]This result is consistent with the results in Ref. 3 where a gluon distribution $xG(x,Q^2=9\ (\mathrm{GeV}/c)^2)\simeq(1-x)^5$ was used. The gluon distribution used here gives a similar result after evolution from $Q^2=4$ to $Q^2=9$ $(\mathrm{GeV}/c)^2$.